

Mechanism of a Novel Metal-Free Carbonic Anhydrase

Shalini Yadav[#], Surajit Kalita^{##} and Kshatresh Dutta Dubey^{*}

Department of Chemistry, School of Natural Sciences, Shiv Nadar Institution of Eminence, Dadri,
Gautam Buddha Nagar, Uttar Pradesh, 201314, India.

Email: kshatresh.dubey@snu.edu.in and surajit.kalita12@gmail.com

Table of Contents

Figure S1: Depiction of bipolar nature of enzyme active site for all2909	S2
S.1. Adaptive Molecular Dynamics Simulation Methodology	S2-S3
Figure S2: Representative MD snapshots and corresponding RMSD plots	S3
S.2. Water Assisted CO ₂ Hydration	S4
Figure S3: Scheme for water assisted CO ₂ hydration and corresponding reaction profile	S4
Figure S4: Proposed schematic pathways for CO ₂ hydration	S5
Figure S5: Occupancy plots of potential proton acceptor amino acids	S5
Figure S6: Radial distribution plot for amino acid around 5 Å from CO ₂ molecule	S6
S.3. Search of well-known proton acceptor residues	S6-S8
Figure S7: QM/MM optimized snapshots and the distance plots	S6
Figure S8: QM/MM explored CO ₂ hydration with His598	S7
Figure S9: QM/MM explored CO ₂ hydration with Glu498	S8
Figure S10: Radial distribution function between Tyr476 and water	S9
Figure S11: QM/MM optimized MD snapshots and corresponding energy profile diagram	S9
QM coordinates of QM/MM Optimized geometries	S10-S13

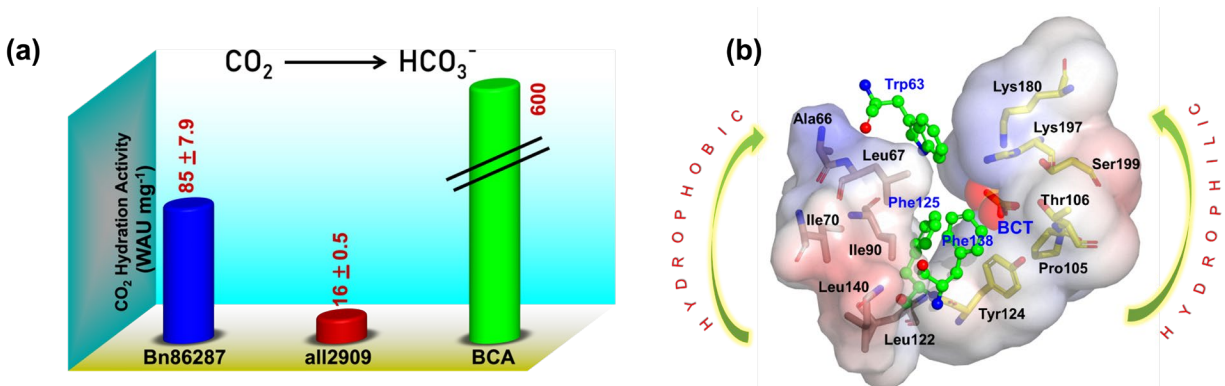


Figure S1: (a) Catalytic activity of CO₂ hydration compared between metal-free CA Bn86287, all2909 and metal dependent bovine carbonic anhydrase. (b) Bipolar nature of the enzyme active site for all2909 (PDB id: 7C5V).

Note that Wilbur-Anderson unit (WAU) is specifically used to measure the activity of carbonic anhydrase enzyme. It is defined as given below:

$$\text{WAU} = (t_0/t) - 1$$

Where, t_0 and t refer to the time taken in the absence and presence of the enzyme, respectively. Higher WAU values directly indicate high activity of the enzyme carbonic anhydrase (CA), reflecting a high turnover number (k_{cat}) and high efficiency.

S.1. Adaptive Molecular Dynamics Simulation Methodology:

To ensure the efficient catalysis in metal free CA enzyme, the exact entrapment zone of tiny CO₂ substrate is important. To explore the feasible route for CO₂ movement, we employed adaptive steered molecular dynamics (ASMD) simulations. For doing so, following the equilibration phase, a pulling force was employed in a predetermined direction and conducted 20 iterative simulations of ASMD. This force was generated by connecting a spring between the center of mass, represented by the ‘C’ atom of CO₂, and a designated ‘OG’ atom of Ser586, which were present at the distance of ~ 3 Å. For doing so we have used a pulling spring force constant (f_0) 10 kcal/mol/Å² with a speed of 1 Å/ns for 320 ns to facilitate the movement of the CO₂ molecule from the hydrophilic zone to the hydrophobic zone. We conducted adaptive steering in 16 stages, progressing along the reaction coordinate from 3 Å to 19 Å up to 320 ns. The process continued

until the substrate CO₂ was completely outside of the hydrophilic zone. Finally, we calculated the potential mean force (PMF), from entire 320 ns of simulation which characterizes the free energy change along a reaction coordinate during different intermediate stages of a CO₂ transition using the Jarzynski's equation.

$$\langle \exp(-\beta W) \rangle = \exp(-\beta \Delta G)$$

In the above equation, $\langle \rangle$ denotes the ensemble average, $\beta = (k_B T)^{-1}$ (k_B is Boltzmann constant and T is temperature; here 300K), W is the work done on the system during a non-equilibrium process, and ΔG is the difference in free energy between two equilibrium states of the system.

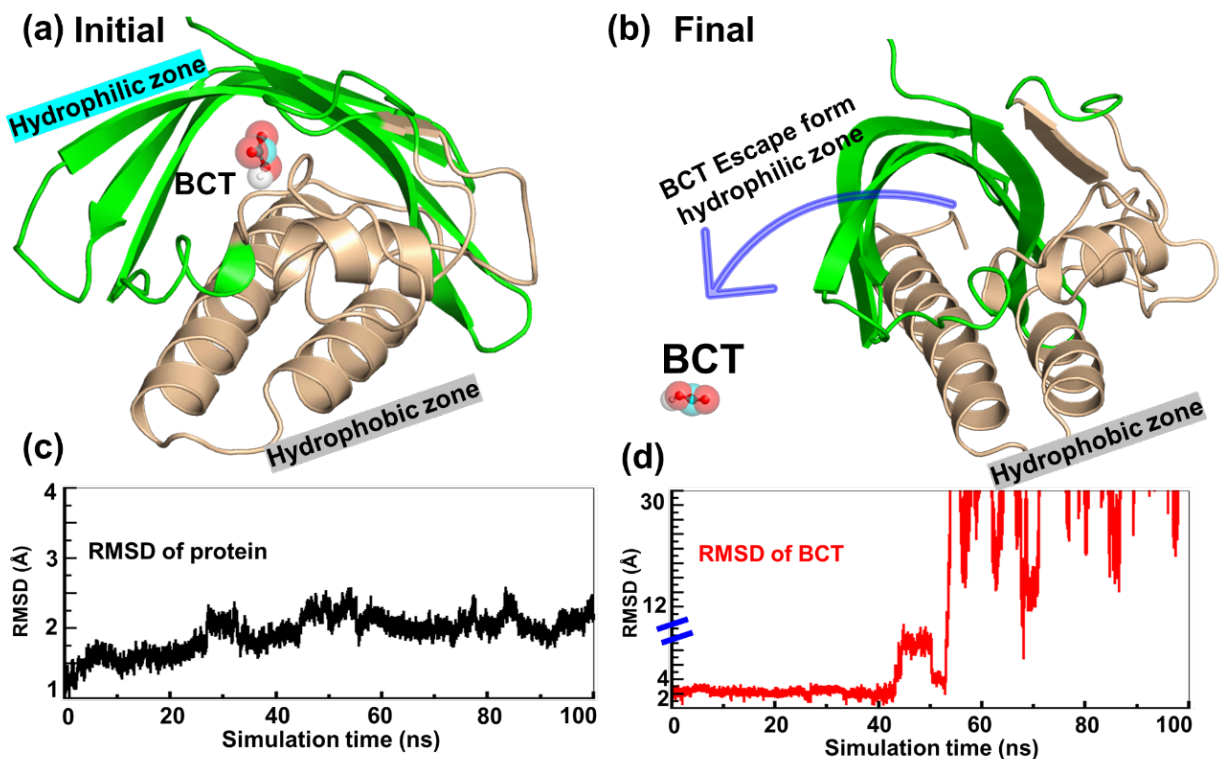


Figure S2: Displaying the outcomes of the MD simulation with HCO₃⁻ (BCT) in the hydrophilic zone. Figures a and b reveal that there is no transfer of the HCO₃⁻ group from the hydrophilic to the hydrophobic region. Instead, it moves away from the hydrophobic cavity after 40 ns of simulation. Figures c and d illustrate the RMSD pattern of the enzyme simulation and the movement of the BCT molecule as it moves away.

S.2. Water Assisted CO₂ Hydration:

As noted in the prior section, the availability of water in the hydrophobic zone is a clearly observable occurrence. Previous research has shown that water facilitates CO₂ hydration, showing that it is a water-mediated process. To check the feasibility of CO₂ conversion to bicarbonate, we first performed DFT-only calculations with CO₂ and two water molecules in the gas phase. Calculation shows a TS barrier of just 21.6 kcal/mol and in a concerted way to form the carbonic acid (H₂CO₃) as a product. Calculation shows the CO₂ gets hydrated to in a concerted manner to form H₂CO₃ (carbonic acid) as a product with a TS barrier of just 21.6 kcal/mol (cf. Figure S1).

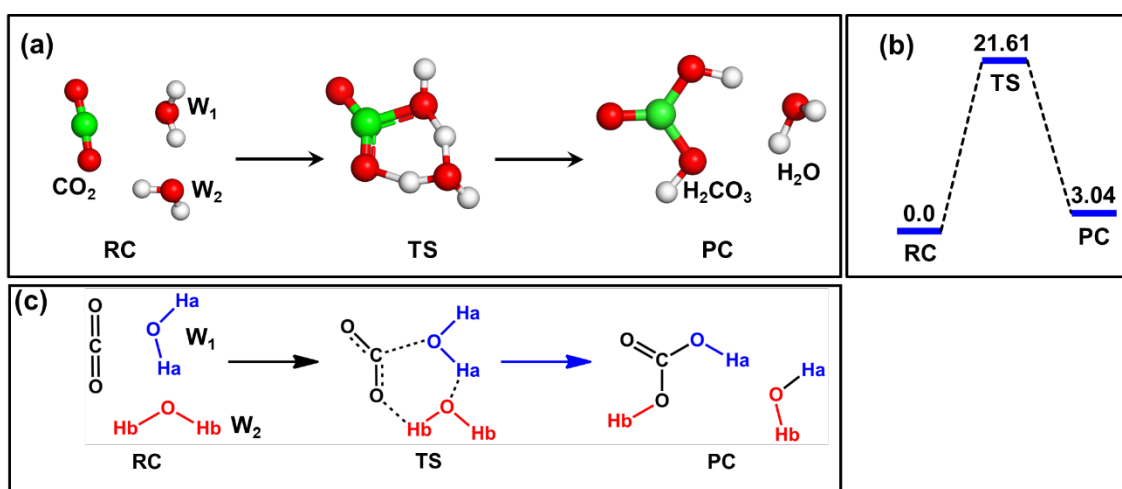
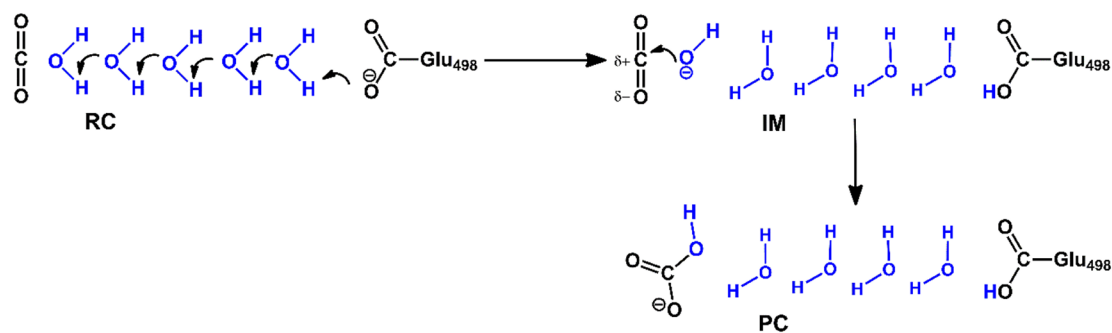


Figure S3: (a) Ball and stick representation of the species involved in the concerted conversion of carbon dioxide into carbonic acid. (b) Gas-phase energy profile diagram for the interconversion of carbon dioxide (RC) into carbonic acid (PC) calculated at the B3LYP/def2-SVP level of theory. Note that energies were further corrected by dispersion correction and zero-point energy correction. The energies are reported in kcal/mol. (c) Concerted mechanism of CO₂ hydration via two water molecules.

By employing two water molecules during the process of CO₂ hydration, we successfully generated H₂CO₃, also known as carbonic acid. This formation, occurring in the gas phase, prompted us to hypothesize the existence of a proton acceptor residue within the hydrophobic zone of the CA enzyme. This residue is expected to play a crucial role in the formation of bicarbonate (H₂CO₃ – H⁺ → HCO₃⁻) by accepting one of the protons involved in the CO₂ hydration reaction in enzymatic environment.

(a) Stepwise Mechanism



(b) Concerted Mechanism

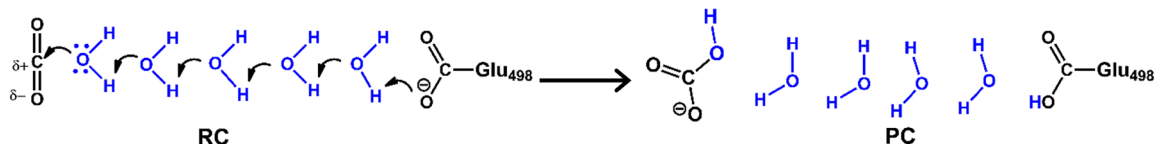


Figure S4. Proposed (a) stepwise and (b) concerted pathways wherein Glutamic acid residue acts as a proton acceptor.

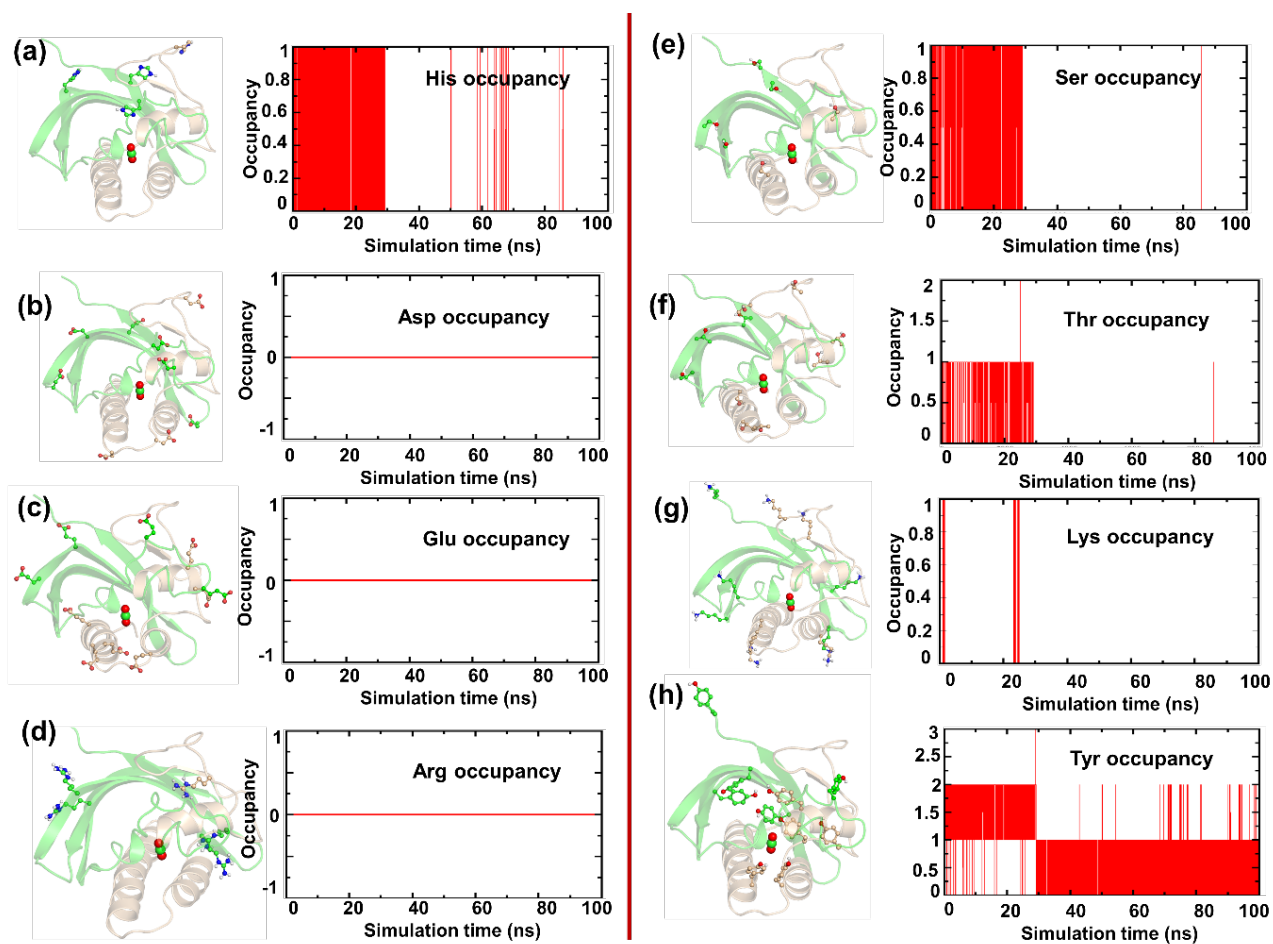


Figure S5: Occupation possibility of different residues calculated near to 5 Å of CO₂ molecule, over the trajectory.

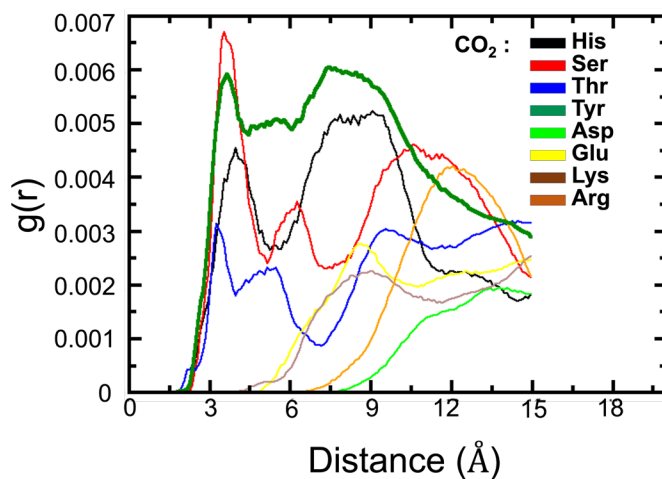


Figure S6: Radial distribution plot for amino acid residues present within 5 Å from CO₂ molecule.

S.3. Proton Acceptor Residues

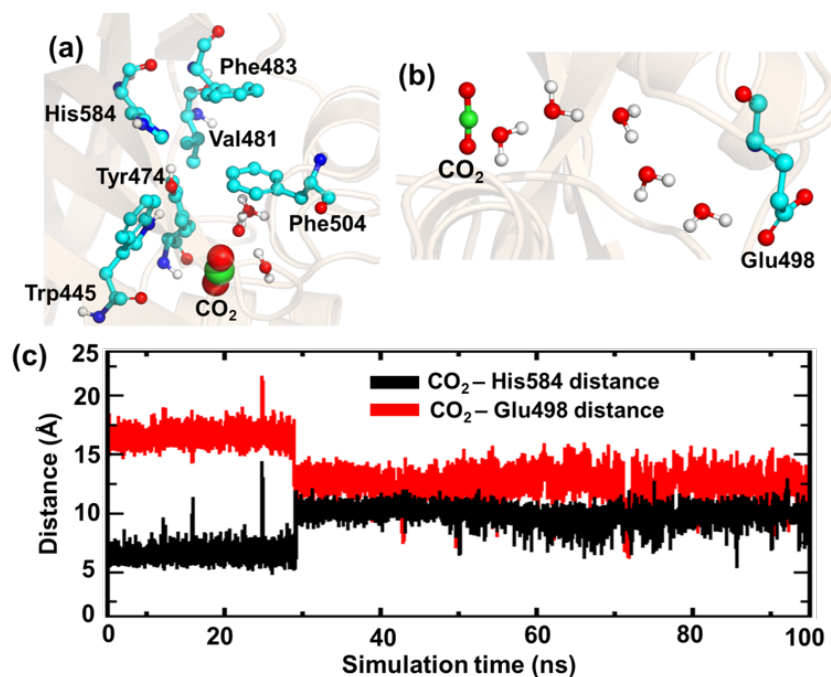


Figure S7. Optimized RC geometry for the proposed pathway for CO₂ hydration; through (a) Histidine (b) Glutamic acid. (c) Distance plot depicts the evolution of positional gap between His584, Glu498 with CO₂.

S.3.a. His584 as a Proton Acceptor Residue:

It is believed that all known metal containing CA enzymes uses histidine residue in their proton shuttle machinery and therefore, we first investigate the role of histidine in the metal independent CA enzyme. A thorough investigation of the MD trajectories reveals that the His584 is located in the hydrophilic zone, which is 8.1 Å away from the CO₂ and sterically hindered by bulky residues. The detailed description can be seen in Figure S5b. In such case, it is almost impossible to abstract a proton by His584 residue from a water molecule that is present nearby CO₂ and therefore, we reject the hypothesis of bicarbonate formation in a concerted way. Thereafter, we attempt to test the stepwise pathway as shown in Figure S6. In this case, two water molecules simultaneously react with the CO₂ molecule, which generates the carbonic acid at a cost of 12.7 kcal/mol energy. Since carbonic acid is an acid molecule, it has a natural tendency to donate its proton to the surroundings. Then, the proton from the carbonic acid is received by the nearby water molecule (W2) and attains the stability by interacting with the adjacent hydroxyl group of the tyrosine residue. Thereafter, the Tyr474 residue relays this additional proton of the water molecule to the nearby His584 residue. Although we obtain a feasible process in our QM/MM derived potential energy surface, the energy cost for the second step of the reaction is very high (>32.9 kcal/mol). Thus, we believe that there must be an alternating low energetic reaction pathway for the efficient catalysis of hydration CO₂ molecule.

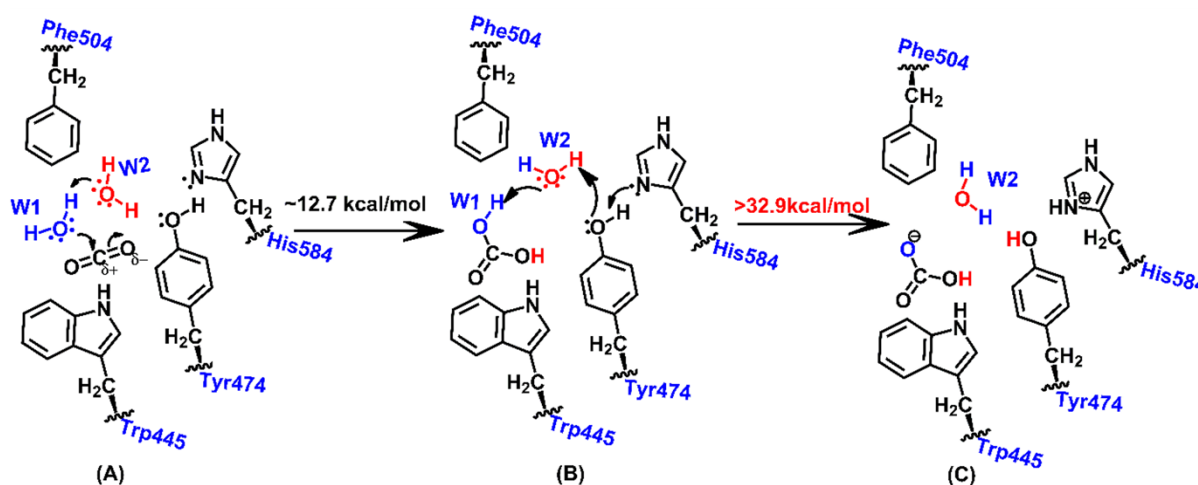
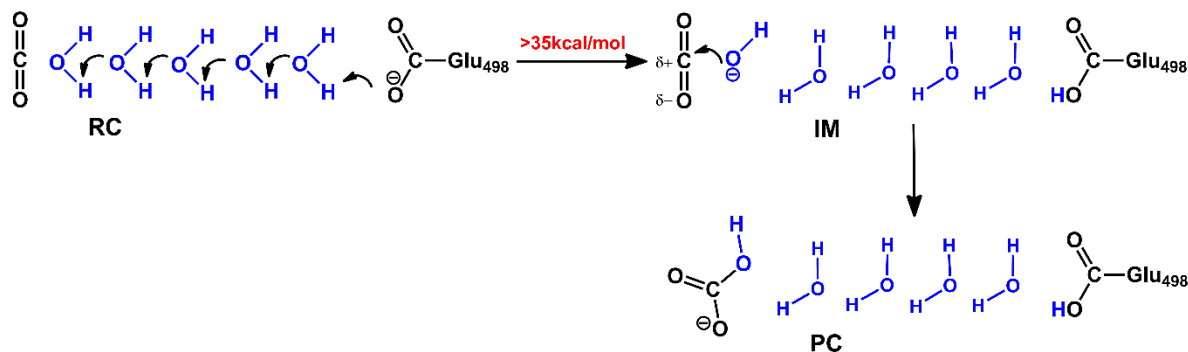


Figure S8. Reaction scheme for CO₂ hydration observed when His acted as a base.

S.3.b. Glu498 as a Proton Acceptor Residue:

Since the traditional proton acceptor, histidine residue requires very high energy to complete the catalytic cycle of the metal independent CA enzyme, we concentrate on the Glu498 as a proton acceptor. As can be seen in Figure S5b, Glu498 residue organizes a water channel connecting to the substrate CO₂ molecule, however the distance between them is very large, which is ~13 Å (cf. S5c).

(a) Stepwise Mechanism



(b) Concerted Mechanism

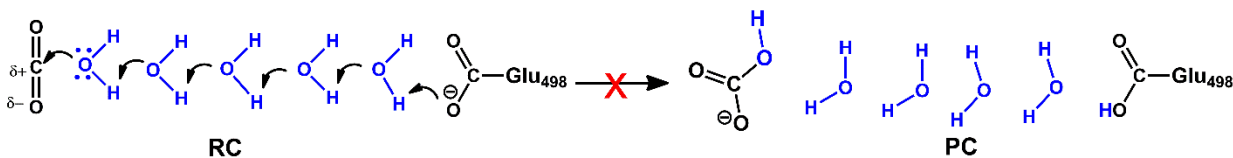


Figure S9. QM/MM explored CO₂ hydration with proton acceptor residue Glu498. We have tested both (a) stepwise and (b) concerted pathways wherein Glutamic acid residue acts as a proton acceptor. However, due to a larger distance between substrate CO₂ and Glu498 (~13.8 Å) the process was not feasible.

Albeit the long distance between the reactive molecules, we have carried out the QM/MM potential energy surface scanning to achieve the product, bicarbonate molecule according to Grotthuss mechanism. Unfortunately, we cannot generate a stable product on the potential energy surface with the help of Glu498 residue. Hence, we reject the idea of Glu498 residue, acting as a proton acceptor residue and further proceeded for the only possibility where Tyr46 acts as a base. (Section 3.7)

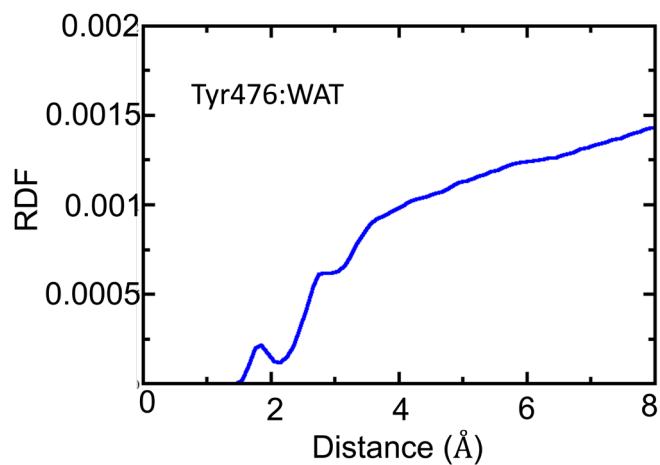


Figure S10: Radial distribution function calculated between residue Tyr476 and water molecules.

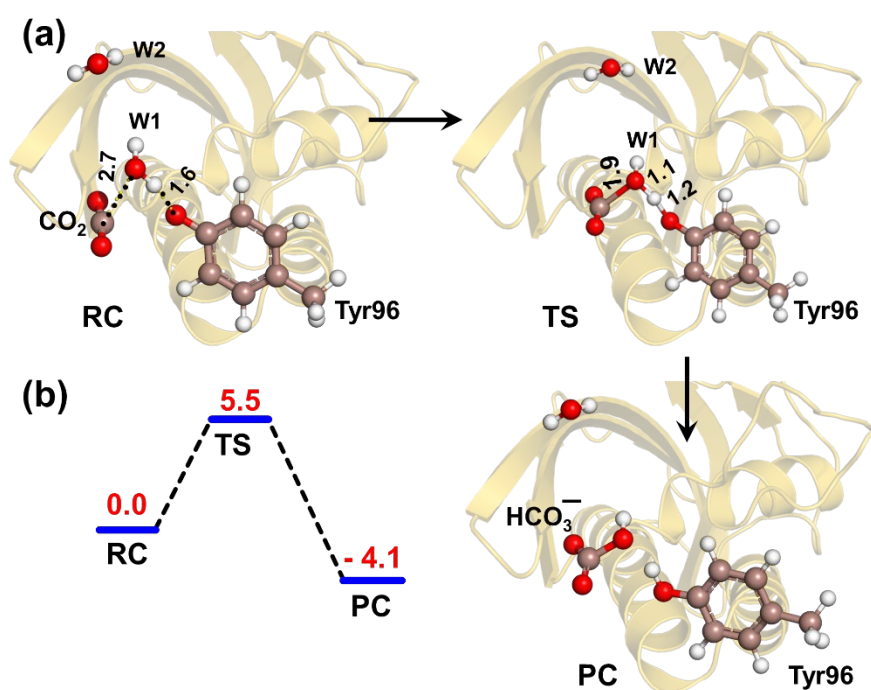


Figure S11: QM/MM optimized geometries involved in the conversion of CO_2 into bicarbonate for all2909. All Energies are in kcal/mol and calculated at B3LYP-D3/def2-TZVP/ZPE level of theory.

**QM Coordinates of optimized geometries
in GAS phase**

RC

C -1.29111200 -0.45204100 -0.00860800
O -2.21512800 0.23982000 0.09778400
O -0.42675400 -1.23328800 -0.10356900
O 2.39592200 -0.42072400 0.17511700
H 2.79136500 -0.59455200 -0.69094200
H 1.60561600 -0.98548700 0.18471700
O 0.45415400 1.55196300 -0.16996800
H 1.27783800 1.04281500 -0.02649200
H 0.40630800 2.14731000 0.58945900

TS

C 0.83978300 -0.20591300 0.02307600
O 2.00142900 0.02947000 -0.09418400
O 0.07074800 -1.17770000 0.08356400
O -2.06813000 -0.04254100 -0.17966800
H -2.57247700 -0.06606200 0.64787200
H -1.28143500 -0.76899100 -0.07970800
O -0.05281300 1.11895700 0.14267300
H -1.21978900 0.77736500 -0.08211200
H 0.42513500 1.86768200 -0.24358900

PC

C -0.87644700 0.07903200 0.00047300
O -2.07373700 0.11410800 0.03855600
O -0.07009500 1.11949600 -0.02769200
O 2.37844500 0.03268300 -0.07119500
H 2.80018400 0.03934500 0.80015000
H 0.88369900 0.83893400 -0.06514800
O -0.17374900 -1.10554800 -0.01595700
H 1.92714800 -0.82706900 -0.11963500
H -0.83926800 -1.81131800 -0.00789900

**Coordinates of QM/MM optimized
geometries for CO₂ hydration in the
Bn86287:**

RC_{Bn86287}

C 18.6988180 30.0411569 34.9654670
H 18.5010893 29.0368978 34.5700140
H 17.8017311 30.6489858 34.7495337
C 19.9423590 30.6044884 34.3140012
C 20.3145099 31.9641602 34.4145558
H 19.6670780 32.6517891 34.9749899
C 21.4637626 32.4672324 33.8170682
H 21.7087085 33.5291472 33.8817239
C 22.3720413 31.6321071 33.0646619
O 23.4537269 32.0692881 32.5480116
C 21.9378013 30.2645446 32.9379413
H 22.5717288 29.6049892 32.3437637

C 20.7834455 29.7800083 33.5475970
H 20.5190047 28.7241496 33.4083899
C 27.5278251 27.0295902 28.5456559
O 26.9187456 26.2855740 29.2060092
O 28.2761086 27.6906507 27.9468858
O 24.1773411 30.5602537 30.5534907
H 23.2684592 30.4919104 30.1818668
H 24.0310510 31.1519219 31.3687001
O 26.0432962 29.3880273 29.1866863
H 25.3307017 29.7578953 29.7994434
H 26.4045735 30.2021383 28.8016016
O 25.4783498 27.7194059 27.1044035
H 25.5284490 28.4005658 27.8210692
H 24.7281470 27.1568836 27.3633833
H 18.7862149 29.9267001 36.0458968

TS_{Bn86287}

C 18.7171848 30.0277458 34.9568998
H 18.5480799 29.0160416 34.5682963
H 17.8095198 30.6127767 34.7254359
C 19.9492977 30.6184245 34.3035332
C 20.2741289 31.9917870 34.3844202
H 19.6161708 32.6599376 34.9548314
C 21.3835102 32.5337628 33.7475380
H 21.5895859 33.6050383 33.7955892
C 22.2847976 31.7295259 32.9604245
O 23.3058259 32.2177908 32.3609304
C 21.9268732 30.3405362 32.8885819
H 22.5821849 29.6942943 32.3007258
C 20.8085302 29.8147104 33.5367617
H 20.5881332 28.7459419 33.4237672

C 27.1241073 27.1168020 28.3413898
O 26.8587307 25.9599458 28.5668293
O 28.0121594 27.9282061 28.3712191
O 23.7532200 31.1317529 30.1320979
H 22.8333052 30.8067464 29.9572521
H 23.6722716 31.5658831 31.0840844
O 25.5892038 29.7312715 29.3300434
H 24.7406575 30.3004051 29.7170979
H 26.2189277 30.3947427 29.0056379
O 25.7329115 27.8972727 27.7710586
H 25.5704518 28.8117191 28.5063422
H 25.0004677 27.2573908 27.8137575
H 18.7942178 29.9227082 36.0390737

PC_{Bn86287}

C 18.7301300 29.9793935 34.9436103
H 18.6839767 28.9501745 34.5708397
H 17.7711972 30.4593518 34.6817162
C 19.8939124 30.7033737 34.2961264
C 20.0866028 32.0883438 34.4530309
H 19.4133457 32.6549825 35.1057332
C 21.0910974 32.7685923 33.7690120
H 21.2073713 33.8508177 33.8592198
C 21.9500210 32.0865551 32.8757742
O 22.8578431 32.7815970 32.1997404
C 21.7905527 30.6886783 32.7435224
H 22.4515317 30.1458491 32.0632102
C 20.7772177 30.0244777 33.4385820
H 20.6499910 28.9479091 33.2796651
C 26.2816476 27.0009368 28.8843683
O 26.7016477 25.9147838 28.4721536

O 26.7212945 27.7835572 29.7501137
O 23.2912383 31.6418412 29.9456556
H 22.3600964 31.3491274 29.7741861
H 23.1319266 32.3017114 31.3448106
O 24.4919565 29.2666529 30.2671805
H 23.8250988 30.8051570 30.0110376
H 25.4451457 28.9980561 30.2817681
O 25.0670640 27.4652062 28.2779404
H 24.2339109 28.7114951 29.5068068
H 24.7094899 26.7199712 27.7695814
H 18.7986044 29.9019074 36.0286791

**QM/MM optimized geometry coordinates
for CO₂ hydration in all2909.**

RC_{all2909}

C 43.6004588 35.6963375 27.3493724
H 43.8792510 34.6690817 27.6348313
H 44.4118691 36.3703328 27.6775102
C 42.2952413 36.0879409 28.0266204
C 41.9326455 37.4381574 28.2234768
H 42.6081125 38.2280313 27.8738031
C 40.7514568 37.8068809 28.8624361
H 40.5104524 38.8653943 29.0004916
C 39.8029396 36.8433059 29.3504292
O 38.6773532 37.1729946 29.8854140
C 40.2267521 35.4803253 29.2033013

H 39.5747045 34.7117737 29.6338724
C 41.4155494 35.1261947 28.5582913
H 41.6839796 34.0634212 28.4800048
C 36.9627163 39.1506881 30.1557401
O 36.7485612 38.9847200 31.2911701
O 37.0800457 39.5089628 29.0532194
O 33.1530041 34.9867582 31.5340955
H 32.9346881 35.8717975 31.8565043
H 33.7477610 34.6085569 32.2308415
O 36.1237667 36.5924134 29.4921687
H 35.8656486 36.1552747 30.3146926
H 37.1208416 36.6714854 29.5848793
H 43.5933079 35.7304311 26.2599443

TS_{all2909}

C 43.6610771 35.6325454 27.3294550
H 43.8911260 34.5839259 27.5746701
H 44.5144674 36.2529614 27.6531739
C 42.4044143 36.0775298 28.0505636
C 42.1621725 37.4406545 28.3163388
H 42.8826224 38.1903937 27.9723573
C 41.0409892 37.8631659 29.0214221
H 40.8759021 38.9246522 29.2258148

C	40.0695136	36.9424624	29.5154990	C	42.6094264	37.6648068	28.3058704
O	39.0383778	37.3545815	30.1944802	H	43.5070150	38.2077404	28.0042738
C	40.3321899	35.5667927	29.2515868	C	41.5961600	38.3579474	28.9530851
H	39.6296713	34.8309550	29.6584061	H	41.6881795	39.4266839	29.1622071
C	41.4664970	35.1554955	28.5437017	C	40.4165291	37.6949072	29.3464401
H	41.6458678	34.0824829	28.3926435	O	39.4781142	38.4187867	29.9572976
C	36.6411794	39.0875410	30.1761669	C	40.3055225	36.3133009	29.0847922
O	36.3695243	39.1242306	31.3342352	H	39.3973565	35.7860325	29.3928564
O	36.8636325	39.5929909	29.1305876	C	41.3463760	35.6289085	28.4421073
O	32.8819067	35.0163691	31.7499940	H	41.2517048	34.5496919	28.2720170
H	32.6196498	35.8691655	32.1223446	C	36.5071580	39.0254958	30.3805672
H	33.5657252	34.6661442	32.3746292	O	36.1984084	39.2400896	31.5603922
O	36.6788755	37.1663916	29.7415801	O	36.5127450	39.6761587	29.3447219
H	36.3394161	36.7397357	30.5411454	O	32.8106780	35.0124517	31.8072591
H	37.8003892	37.1295580	29.8938321	H	32.6324728	35.9193387	32.0900145
H	43.6169114	35.7063276	26.2428673	H	33.5338109	34.6920753	32.4002627
PC_{all2909}				O	36.9829576	37.6219638	30.1677137
C	43.6549773	35.5881201	27.3247671	H	36.8684369	37.2348012	31.0483365
H	43.6975859	34.5158856	27.5742382	H	38.5892155	37.9686054	30.0090439
H	44.6035888	36.0457081	27.6473003	H	43.6117826	35.6813701	26.2396377
C	42.5113060	36.2888402	28.0279360				

